Characteristics Method Using Cubic–Spline Interpolation for Advection–Diffusion Equation

Tung-Lin Tsai[1]; Jinn-Chuang Yang, M.ASCE[2]; and Liang-Hsiung Huang, A.M.ASCE[3]

Abstract: The characteristics method by using the cubic-spline interpolation is comparable to the Holly–Preissmann scheme in solving the advection portion of the advection–diffusion equation. In order to conduct a cubic-spline interpolation, an additional constraint must be specified at each endpoint. In general, four types of endpoint constraints are available, i.e., the first derivative, second derivative, quadratic, and not-a-knot constraints. The goal of this paper is to examine each type of endpoint constraints. Two hypothetical cases are used to conduct the investigation. Among the four types of constraints examined herein, the not-a-knot constraint and the first derivative constraint with high-order finite difference approximation yield the best results. However, as far as accuracy and simple implementation are concerned the not-a-knot constraint should be the best choice in solving the advection–diffusion equation

DOI: 10.1061/(ASCE)0733-9429(2004)130:6(580)

CE Database subject headings: Advection; Diffusion; Interpolation.

Introduction

The advection–diffusion equation is one of the governing equations in solving mass transport in river, lakes, oceans, and groundwater. A variety of numerical methods are available to solve the advection–diffusion equation. However, none of them is considered satisfactory. Yet the primary difficulty arises from the combined hyperbolic (advection) and parabolic (diffusion) nature. The split-operator approach in which the advection and diffusion processes are separately computed using different numerical schemes has been pursued by many numerical modelers. In the split-operator approach, since the diffusion process can be accurately computed by several numerical methods, such as the Crank–Nicholson central difference scheme, the Crank–Nicholson Galerkin finite element method, and some others. Hence, the accuracy of solving the advection–diffusion equation will mainly depend on the computed results of the advection process.

The characteristics-based Holly–Preissmann scheme (Holly and Preissmann 1977) with a fourth-order Hermitic interpolation between grid points is considered one of the best methods because of less numerical oscillation and damping in modeling the advection process. The Holly–Preissmann scheme was successfully applied to a number of hydraulic problems (Holly and Usseglio-Polatera 1984; Toda and Holly 1987; Holly and Rahuel 1990; Yang and Hsu 1991). It was further examined by Glass and Rodi (1982). In spite of all the successes, the Holly–Preissmann scheme achieves its high accuracy at the expense of lengthy computation time for tackling spatial derivatives with auxiliary equations. To obviate the need of solving the first spatial derivatives of the auxiliary equation, an alternative with the use of cubic-spline interpolation function was proposed by Schohl and Holly (1991), Karpik and Crokett (1997), and Stefanovic and Stefan (2001). The cubic-spline interpolation with the accuracy comparable to the Hermitic interpolation may achieve some reduction in computational time and memory.

The cubic-spline interpolation function must pass through each given data location (or node) and be continuous in its first and second derivatives at interior nodes. Thus, it is necessary to specify two additional endpoint (i.e., upstream and downstream boundaries) constraints. In general, there exist four different types of endpoint constraints, i.e., first derivative, second derivative, quadratic, and not-a-knot endpoint constraints (e.g., Gerald and Wheatley 1994; Knott 1999; Kvasov 2000). The natural cubic-spline interpolation with neglect of second derivative at the endpoints is most frequently used (e.g., Schohl and Holly 1991; Karpik and Crokett 1997; Stefanovic and Stefan 2001). However, in all their cases, the computational domains are so large that the influences of boundary are irrelevant, and therefore any type of endpoint conditions may obtain the same result. Further, the natural cubic-spline interpolation may yield the end cubics to approach linearity at their extremities and flatten the interpolating curve too much due to neglect of second derivative at endpoints. The main goal of this paper is to examine which type of endpoint constraints in solving the advection–diffusion equation is the best, especially when the influences of boundary are not negligible.

Numerical Framework of Advection–Diffusion Simulation

The one-dimensional advection–diffusion equation can be expressed as

$$\frac{\partial \Phi}{\partial t} + U \frac{\partial \Phi}{\partial x} = D \frac{\partial^2 \Phi}{\partial x^2} \tag{1}$$

[1]Research Assistant Professor, Natural Hazard Mitigation Research Center, National Chiao Tung Univ., Hsinchu, Taiwan 30010, R.O.C.

[2]Professor, Dept. of Civ. Engrg., National Chiao Tung Univ., Hsinchu, Taiwan 30010, R.O.C.

[3]Professor, Dept. of Civ. Engrg., National Taiwan Univ., Taipei, Taiwan 10617, R.O.C.

Note. Discussion open until November 1, 2004. Separate discussions must be submitted for individual papers. To extend the closing date by one month, a written request must be filed with the ASCE Managing Editor. The manuscript for this technical note was submitted for review and possible publication on November 12, 2002; approved on October 30, 2003. This technical note is part of the ***Journal of Hydraulic Engineering***, Vol. 130, No. 6, June 1, 2004. ©ASCE, ISSN 0733-9429/2004/6-580–585/$18.00.

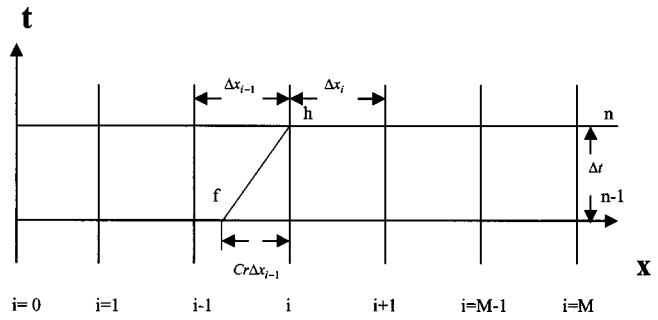

Fig. 1. Schematic grid diagram for cubic-spine interpolation

where the scalar function $\Phi(x,t)$ may represent, for example, temperature or concentration at position x and time t with flow velocity U and diffusion coefficient D. By applying the split-operator approach (Yanenko 1968; Sobey 1984; Holly and Ussglio-Polatera 1984; Lin and Falconer 1997), Eq. (1) may be approximated with combination of two kinds of transport processes: a pure advection process described by

$$\frac{\partial \Phi}{\partial t}+U\frac{\partial \Phi}{\partial x}=0 \tag{2}$$

and a pure diffusion process written as follows:

$$\frac{\partial \Phi}{\partial t}=D\frac{\partial^2 \Phi}{\partial x^2} \tag{3}$$

The advantage of the split-operator approach is that it makes the choice of the most appropriate scheme for each transport process, whereas the disadvantage is the violation of the fact that advection and diffusion occur simultaneously.

Solution of Advection Process

The characteristics method with interpolating approximation of solution is widely used for solving the advection process. Eq. (2) can be written in terms of total derivative, i.e., D_s/Dt, as

$$\frac{D_s \Phi}{Dt}=0 \tag{4}$$

along

$$\frac{dx}{dt}=U \tag{5}$$

Integration of the above equations yields

$$\Phi_h=\Phi_f \tag{6}$$

along

$$x_h-x_f=U\Delta t=\mathrm{Cr}\Delta x \tag{7}$$

where Δx and Δt represent the grid size and time step, respectively (see Fig. 1). Cr is the Courant number. The schematic diagram of the characteristic trajectory is shown in Fig. 1. Φ_h is the unknown concentration of grid point h at time level n, which is to be solved. Φ_f is the concentration of grid point f at time level $n-1$, in which concentrations of all grid points are known. Since, in general, the foot of the trajectory, x_f, does not coincide with grid points, one must employ some form of interpolation to obtain the required concentration, Φ_f. Thus, the accuracy of the solution is significantly related to the choice of the interpolation function.

One may develop a cubic-spline interpolation function for evaluating Φ_h corresponding to all the known concentrations at time level $n-1$, that is, Φ_i^{n-1}, $i=0,1,...,M$ shown in Fig. 1. In the cubic-spline interpolation, the second derivative is a continuous piecewise linear function and can be expressed as

$$\Phi^{n-1}(x)''=S_1\frac{x_{i+1}-x}{\Delta x_i}+S_{i+1}\frac{x-x_i}{\Delta x_i},\quad x\in[x_i,x_{i+1}] \tag{8}$$

where $\Delta x_i=x_{i+1}-x_i$, $i=0,...,M-1$; x_i is the coordinate of grid point; $\Phi^{n-1}(x)''$ denotes the function of second derivative of concentration; and S_i and S_{i+1} represent the second derivative at grid points i and $i+1$, respectively. Integrating Eq. (8) twice and substituting the values of concentrations at grid points i and $i+1$ yields the expression for the cubic function $\Phi^{n-1}(x)$ on $[x_i,x_{i+1}]$ as follows:

$$\Phi^{n-1}(x)=S_i\frac{(x_{i+1}-x)^3}{6\Delta x_i}+S_{i+1}\frac{(x-x_i)^3}{6\Delta x_i}+\left(\Phi_i^{n-1}-S_i\frac{\Delta x_i^2}{6}\right)\times\frac{x_{i+1}-x}{\Delta x_i}+\left(\Phi_{i+1}^{n-1}-S_{i+1}\frac{\Delta x_i^2}{6}\right)\frac{x-x_i}{\Delta x_i} \tag{9}$$

The second derivative of grid points, S_i, in Eq. (9) can be found by applying the continuity of the first derivative at interior nodes as follows:

$$\Delta x_{i-1}S_{i-1}+2(\Delta x_{i-1}+\Delta x_i)S_i+\Delta x_i S_{i+1}=6\left(\frac{\Phi_{i+1}^{n-1}-\Phi_i^{n-1}}{\Delta x_i}-\frac{\Phi_i^{n-1}-\Phi_{i-1}^{n-1}}{\Delta x_{i-1}}\right),\quad i=1,...,M-1 \tag{10}$$

The system of Eq. (10) is underdetermined as it contains only $M-1$ equations for finding $M+1$ unknowns. To complete this system two additional constraints (i.e., two endpoint constraints) for S_0 and S_M are required. Four types of endpoint constraints (Gerald and Wheatley 1994; Knott 1999; Kvasov 2000) may be used to produce the various types of cubic-spline interpolations. They are stated below.

1. First derivative endpoint constraints,

$$2\Delta x_0 S_0+\Delta x_1 S_1=6\left(\frac{\Phi_1^{n-1}-\Phi_0^{n-1}}{\Delta x_0}-\frac{\partial \Phi(x_0)}{\partial x}\right) \tag{11a}$$

and

$$2\Delta x_{M-1}S_M+\Delta x_{M-2}S_{M-1}=6\left(\frac{\partial \Phi(x_M)}{\partial x}-\frac{\Phi_M^{n-1}-\Phi_{M-1}^{n-1}}{\Delta x_{M-1}}\right) \tag{11b}$$

2. Second derivative endpoint constraints,

$$S_0=\frac{\partial^2 \Phi(x_0)}{\partial x^2}\quad \text{and}\quad S_M=\frac{\partial^2 \Phi(x_M)}{\partial x^2} \tag{12}$$

3. Quadratic endpoint constraints,

$$S_0=S_1\quad \text{and}\quad S_M=S_{M-1} \tag{13}$$

4. Not-a-knot endpoint constraints,

$$S_0=\frac{(\Delta x_0+\Delta x_1)S_1-\Delta x_0 S_2}{\Delta x_1}$$

and

$$S_M=\frac{(\Delta x_{M-2}+\Delta x_{M-1})S_{M-1}-\Delta x_{M-1}S_{M-2}}{\Delta x_{M-2}} \tag{14}$$

In Eqs. (11) and (12), the unknown first and second derivatives could be obtained by finite difference approximation corresponding to grid points near the boundary. However, the frequently

Table 1. Root Mean Square Error of Various Endpoint Constraints in Pure Advection Test

	$\Delta x^*=0.02$			$\Delta x^*=0.025$			$\Delta x^*=0.01$		
	0.3	0.6	0.9	0.9	0.6	0.9	0.3	0.6	0.9
Natural	0.0571	0.0372	0.0079	0.0963	0.0637	0.0136	0.0088	0.0077	0.0017
Quadratic	0.0397	0.0244	0.0034	0.0805	0.0453	0.0069	0.0034	0.0026	0.0004
Not-a-knot	0.0191	0.0099	0.0009	0.0475	0.0203	0.0023	0.0018	0.0012	0.0001
First derivative	0.0717	0.0120	0.0198	0.1140	0.0795	0.0198	0.0125	0.0111	0.0028
1st order	0.0717	0.0120	0.0198	0.1140	0.0795	0.0198	0.0125	0.0111	0.0028
2nd order	0.0473	0.0048	0.0096	0.0931	0.0544	0.0096	0.0041	0.0032	0.0006
3rd order	0.0222	0.0012	0.0033	0.0571	0.0268	0.0033	0.0018	0.0011	0.0001
4th order	0.0135	0.0016	0.0037	0.0237	0.0163	0.0037	0.0019	0.0015	0.0002
5th order	0.0222	0.0022	0.0054	0.0413	0.0295	0.0054	0.0020	0.0017	0.0002
Second derivative									
1st order	0.0442	0.0042	0.0085	0.0880	0.0507	0.0085	0.0037	0.0029	0.0005
2nd order	0.0218	0.0012	0.0031	0.0585	0.0262	0.0031	0.0018	0.0012	0.0001
3rd order	0.0413	0.0046	0.0075	0.0680	0.0437	0.0075	0.0062	0.0052	0.0009
4th order	0.0480	0.0053	0.0096	0.0815	0.0525	0.0096	0.0067	0.0056	0.0010

Note: Δx^*=grid size and Courant number=Cr=0.3, 0.6, and 0.9.

used natural cubic-spline interpolation simply takes $S_0=S_M=0$ in Eq. (12) and neglects the second derivative at endpoints. Thus, it makes the end cubics approach linearity at their extremities. On the other hand, by substituting Eq. (13) into Eq. (9), one can clearly find that this endpoint constraint is equivalent to assuming that the end cubics approach to quadratic curves at their extremities. The not-a-knot endpoint constraint as shown in Eq. (14) represents the continuity of the third derivative at the nodes x_1 and x_{M-1} (de Boor 1978). In other words, two cubic segments that join at the node x_1 are adjacent parts of the same cubic curve. The identical result as that at node x_1 is also yielded at node x_{M-1}.

Solution of Diffusion Step

The second step in the split-operator approach is the diffusion transport of the advected concentration field as shown in Eq. (3). The computation of the diffusion process can be accurately executed by using a variety of finite-difference and finite-element numerical schemes. The Crank–Nicholson second-order central difference scheme is used here. The discretized equation (3) for a uniform grid size can be written as

$$\frac{\Phi_i^{n+1}-\Phi_a}{\Delta t}=\frac{D}{2\Delta x^2}[(\Phi_{i+1}^{n+1}-2\Phi_i^{n+1}+\Phi_{i-1}^{n+1}) + (\Phi_{i+1}^{n}-2\Phi_i^{n}+\Phi_{i-1}^{n})] \quad (15)$$

where Φ_a is a value of concentration obtained from the advection process at i point. This would form a tridiagonal system of algebraic equations, which can be solved by the efficient Thomas algorithm.

Evaluation of Different Endpoint Constraints

Calculation of Transport of Sine Function

To investigate the computational performances of cubic-spine interpolation with different endpoint constraints, a nondimensional advection–diffusion equation with uniform flow velocity, U, and diffusion coefficient, D, is considered as follows:

$$\frac{\partial \Phi^*}{\partial t^*}+\frac{\partial \Phi^*}{\partial x^*}=\frac{1}{\mathrm{P}}\frac{\partial^2 \Phi^*}{\partial x^{*2}} \quad (16)$$

where $\Phi^*=\Phi/\Phi^0$, $x^*=x/L$, $t^*=Ut/L$ are nondimensional concentration, coordinate, and time; Φ_0 and L are characteristic concentration and length, respectively; and $\mathrm{P}=UL/D$ represents Péclet number.

Under the initial condition

$$\Phi^*(x^*,t^*=0)=\sin(2\omega\pi x^*) \quad (17)$$

and the boundary conditions

$$\Phi^*(x^*=0,t^*)=\sin(-2\omega\pi t^*)\exp(-4\pi^2\omega^2 t^*/\mathrm{P}) \quad (18)$$

$$\Phi^*(x^*=1,t^*)=\sin 2\omega\pi(1-t^*)\exp(-4\pi^2\omega^2 t^*/\mathrm{P}) \quad (19)$$

the exact solution to (16) is

$$\Phi^*(x^*,t^*)=\sin 2\omega\pi(x^*-t^*)\exp(-4\pi^2\omega^2 t/\mathrm{P}) \quad (20)$$

where ω represents the periodical number of sine function in the computational domain. In this study, $\omega=5$ is used.

First, the pure advection equation (i.e., $\mathrm{P}\to\infty$) is considered. Numerical results in terms of root mean square (rms) error with different Courant numbers and uniform grid of 0.02, 0.025, and 0.01 for 200 time steps by the natural, quadratic, and not-a-knot constraints as well as the first and second derivative constraints with different order finite difference approximation are, respectively, given in Table 1. Fig. 2 shows the simulated results of various constraints with Courant number of 0.3 and uniform grid of 0.025. It is observed that the natural constraint induces larger rms error and numerical diffusion than the other constraints, excluding the first derivative constraint with first order finite difference approximation. This may be because the natural cubic-spline interpolation flattens the interpolating curve too much at the ends due to the assumption of neglecting second order derivative at endpoints, which makes the end cubics approach linearity at their extremities. The simulated results of not-a-knot constraint are better than those of the quadratic constraint.

It is clearly found that the results of the first and second derivative endpoint constraints depend on the derivative approximations, especially for the former constraint. However, the more

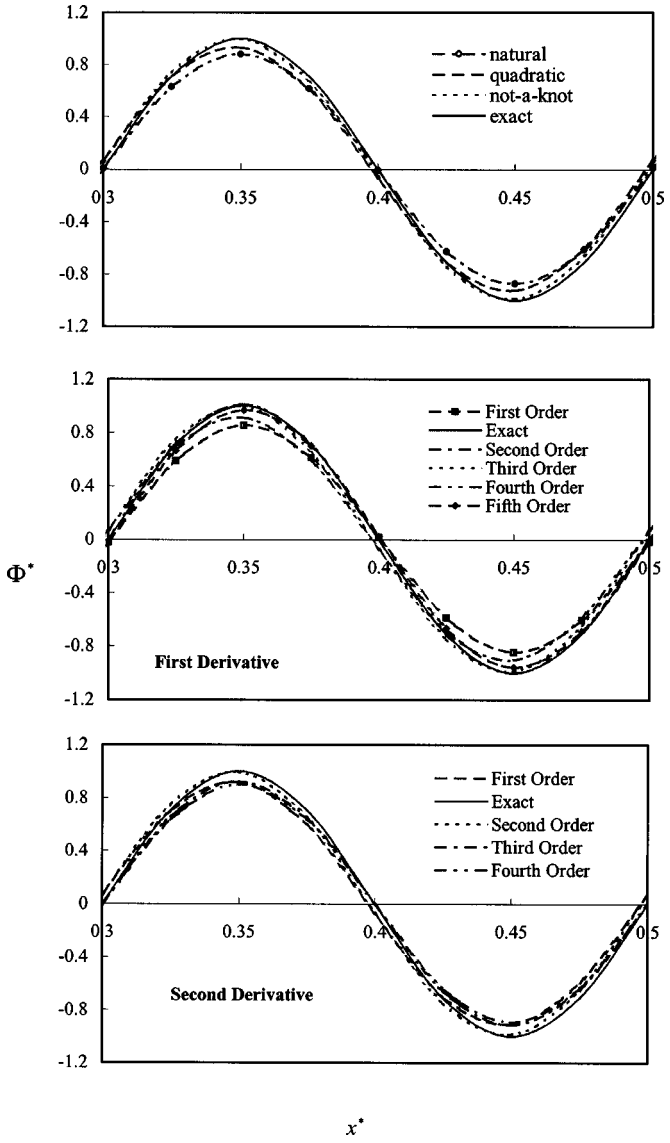

Fig. 2. Computational results of various endpoint constraints for pure advection equation ($\Delta x^* = 0.025$, $Cr = 0.3$)

accurate derivative approximations may not yield better results. The first and second derivative endpoint constraints seem to have better results when the fourth and second order finite difference approximations are applied, respectively. This may be due to the inconsistency of accuracy between the derivative approximations and the cubic-spline interpolation. For the first derivative endpoint constraint, the first order finite difference approximation produces larger numerical damping than the natural constraint. The second order finite difference approximation has worse simulated results than the quadratic constraint. The simulated results of the third and higher order finite difference approximations are comparable to those of the not-a-knot constraint. On the other hand, the second derivative constraint with finite difference approximation has similar simulated results in comparison with the quadratic constraint. In addition, one can find from Table 1 that the accuracy of simulated results for all the endpoint constraints increases significantly when the grid size decreases from 0.025 to 0.01.

For the advection–diffusion equation, the computational results of different endpoints constraints for 100 time steps and

Table 2. RMS Error of Various Endpoint Constraints for Advection-Diffusion Equation ($\Delta x^* = 0.025$, $Cr = 0.6$)

	Peclet number	
	$1/P = 0.0002$	$1/P = 0.002$
Natural	0.0445	0.0014
Quadratic	0.0310	0.0011
Not-a-knot	0.0144	0.0012
First derivative		
1st order	0.0563	0.0023
2nd order	0.0378	0.0013
3rd order	0.0179	0.0014
4th order	0.0101	0.0014
5th order	0.0194	0.0010
Second derivative		
1st order	0.0350	0.0012
2nd order	0.0175	0.0014
3rd order	0.0296	0.0005
4th order	0.0362	0.0010

$Cr = 0.6$ are shown in Table 2 for $1/P = 0.0002$ and $1/P = 0.002$, respectively. For large Péclet number (i.e., the advection dominates the transport process) the performances of simulated results by all the constraints are similar to those of pure advection equation mentioned above. However, for small Péclet number, all the constraints yield comparable results that are better than those of large Péclet number.

In this example, one can find that the natural constraint induces large numerical damping and rms error among those constraints considered. The simulated results of the quadratic and second derivative constraints with finite difference approximation are comparable. The not-a-knot constraint and the first derivative constraint with high-order finite difference approximation seem to have the best results in comparison with the other constraints. Since the results of the first derivative constraint are strongly related to the derivative approximation, as far as accuracy and simple implementation are concerned one may conclude that the not-a-knot constraint should be the best choice for solving the advection–diffusion equation by characteristics method with cubic-spline interpolation. In the following example, further examination of the natural constraint and not-a-knot constraint for the transport of Gaussian distribution are conducted.

Calculation of Transport of Gaussian Distribution

With the following initial condition,

$$\Phi(x) = \exp\left[\frac{-(x-x_1)^2}{2\sigma^2}\right] + \exp\left[\frac{-(x-x_2)^2}{2\sigma^2}\right] \tag{21}$$

the solution of (1) is

$$\Phi(x,t) = \frac{\sigma}{\sqrt{\sigma^2+2Dt}}\left\{\exp\left[\frac{-(x-x_1-Ut)^2}{2(\sigma^2+2Dt)}\right] + \exp\left[\frac{-(x-x_2-Ut)^2}{2(\sigma^2+2Dt)}\right]\right\} \tag{22}$$

where σ=standard deviation of Gaussian distribution; and x_1 and x_2 represent the locations of peaks of Gaussian distribution.

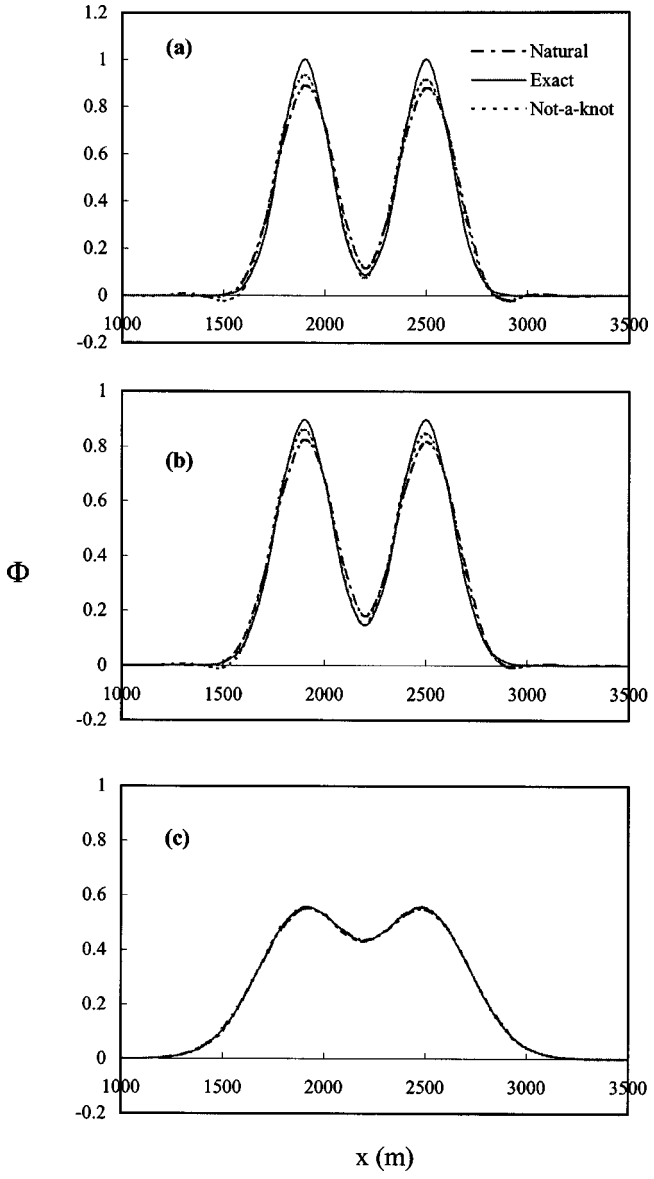

Fig. 3. Computational results of Gaussian distribution for natural and not-a-knot endpoint constraints ($U=0.7$ m/s, $\Delta x=100$ m, $\Delta t=100$ s): (a) $D=0$ m^2/s, (b) $D=0.35$ m^2/s, (c) $D=3.5$ m^2/s

In this problem, the computational domain is $x\in[0,x^b]$, x^b is the location of downstream boundary where the domain of simulation is long enough so that the boundary effect can be ignored. A grid size of 100 m, a time step of 100 s, and a standard deviation of 120 m are used to conduct the simulation. The Gaussian distribution is advected for 50,000 s under a constant flow velocity $U=0.7$ m/s. The two peak positions of this Gaussian distribution are at $x_1=-1000$ m and $x_2=-1600$ m, respectively. Thus, one can know that the Gaussian distribution is out of computational domain in the beginning of simulation. With the transport process, the Gaussian distribution passes through the upstream boundary ($x=0$) into the computational domain.

Numerical results by the natural and not-a-knot constraints are shown in Fig. 3 for $D=0$, 0.35, and 3.5 m^2/s, respectively. Fig. 3 demonstrates that for the advection dominated transport the natural constraint induces larger numerical damping than the not-a-knot constraint. In spite of a little numerical oscillation, the not-a-knot constraint has better simulated results in comparison with the natural condition. However, for the large diffusion coefficient, the computational results by the two constraints are almost identical to the exact solution. So, from the overall examination, the not-a-knot constraint should be suggested to replace the frequently used natural constraint as an alternative for solving the advection–diffusion equation by characteristics method with cubic-spline interpolation.

Conclusions

The cubic-spline interpolation function not only needs to pass through each given data node but also needs to be continuous in its first and second derivatives at interior nodes, an additional constraint must therefore be specified at each endpoint. In general, the first derivative, second derivative, quadratic, and not-a-knot constraints are four different types of endpoint constraints. Two hypothetical cases for transport of sine function and Gaussian distribution are used to investigate each type of constraint. The results show that the frequently used natural constraint induces larger numerical damping and rms error than the other constraints. The quadratic constraint and the second derivative constraint with finite difference approximation have comparable results. It is also found that the results of the first derivative constraint strongly depend on the derivative approximation. The not-a-knot constraint and the first derivative constraint with higher order finite difference approximation seem to have the best results in comparison with the other constraints. In conclusion, as far as accuracy and simple implementation are concerned the not-a-knot constraint should be the best choice in solving the advection–diffusion equation.

Notation

The following symbols are used in this technical note:

Cr = Courant number;
D = diffusion coefficient;
L = characteristic length;
P = Péclet number;
S = second derivative;
U = flow velocity component;
Δx = computational grid interval;
Δt = time increment;
σ = standard deviation;
Φ = concentration;
Φ_0 = characteristic concentration;
Φ^* = nondimensional concentration; and
ω = periodical number of sine function in the computational domain.

Subscripts

i = x-directional computational point index.

Superscripts

n = time step index.

References

DeBoor, C. (1978). *A practical guide to spline*. Springer, New York.
Gerald, C. F., and Wheatley, P. O. (1994). *Applied numerical analysis*. Addison-Wesley, New York.

Glass, J., and Rodi, W. (1982). ''A higher order numerical scheme for scalar transport.'' *Comput. Methods Appl. Mech. Eng.*, 31, 337–358.
Holly, F. M., Jr., and Preissmann, A. (1977). ''Accurate calculation of transport in two dimensions.'' *J. Hydraul. Div., Am. Soc. Civ. Eng.*, 103(11), 1259–1277.
Holly, F. M., Jr., and Usseglio-Polatera, J. (1984). ''Dispersion simulation in two-dimensional tidal flow.'' *J. Hydraul. Eng.*, 110(7), 905–926.
Holly, F. M., Jr., and Rahuel, J. L. (1990). ''New numerical/physical framework for mobile-bed modeling, part I-Numerical and physical principles.'' *J. Hydraul. Res.*, 28(4), 401–416.
Karpik, S. R., and Crockett, S. R. (1997). ''Semi-Lagrangian algorithm for two-dimensional advection-diffusion equation on curvilinear coordinate meshes.'' *J. Hydraul. Eng.*, 123(5), 389–401.
Knott, G. D. (1999). *Interpolating cubic splines*. Birkhauser, Boston.
Kvasov, B. I. (2000). *Shape-preserving spline approximation*. Scientific Publishing, Singapore.
Lin, B., and Falconer, R. A. (1997). ''Tidal flow and transport modeling using ULTIMATE QUICKEST scheme.'' *J. Hydraul. Eng.*, 123(4), 303–314.
Schohl, G. A., and Holly, F. M., Jr. (1991). ''Cubic-spline interpolation in Lagrangian advection computation.'' *J. Hydraul. Eng.*, 117(2), 248–253.
Sobey, R. J. (1984). ''Numerical alternatives in transient stream response.'' *J. Hydraul. Eng.*, 110(6), 749–772.
Stefanovic, D. L., and Stefan, H. G. (2001). ''Accurate two-dimensional simulation of advective-diffusive-reactive transport.'' *J. Hydraul. Eng.*, 127(9), 728–737.
Toda, K., and Holly, F. M., Jr. (1987). ''Hybrid numerical method for linear advection-diffusion.'' *Microsoftw. Eng.*, 3(4), 199–205.
Yang, J. C., and Hsu, E. L. (1991). ''On the use of the reach-back characteristics method for calculation of dispersion.'' *Int. J. Numer. Methods Fluids*, 12, 225–235.
Yaneko, N. N. (1971). *The method of fractional steps: The solution of problems of mathematical physics in several variables*, Springer, New York.